The Importance of Ligand Kinetic Basicity on the Preparation of Surface-Supported Zirconium Complexes by Proton Transfer from Hydroxylated Aluminum or Silicon

John B. Miller, Jeffrey Schwartz,* and Steven L. Bernasek

Contribution from the Department of Chemistry, Princeton University, Princeton, New Jersey 08544-1009

Received April 29, 1993⊛

Abstract: Surface hydroxylation of Al or Si powders or thin films was readily accomplished under various conditions of oxidation vigor. In the first, the metal was exposed to ambient water; in the second, it was immersed in liquid water; in the third, it was treated with steam. Hydroxylation using D_2O steam was also accomplished. Metal surfaces thus activated were examined using various spectroscopic techniques including IR and Auger spectroscopies. The reaction between tetraneopentylzirconium or tetra-*tert*-butoxyzirconium was studied with variously hydroxylated Si or Al. Rates for reaction between the organometallic and surface hydroxyls were studied gravimetrically using the quartz crystal microbalance. Measured kinetic isotope effects suggest a mechanism for organometallic complex surface hydroxyl reactivity involving reversible coordination followed by rate-determining proton transfer. Deposition rates and kinetic isotope effects for the two complexes are discussed in terms of kinetically likely sites for protonation of the two complexes. A simplistic approach, based solely on relative thermodynamic basicities of the two complexes, fails to correctly predict relative reactivities for the two species: tetra-*tert*-butoxyzirconium is *ca.* an order of magnitude more reactive, ratewise, than is the more thermodynamically basic tetraneopentylzirconium.

Introduction

Dehydration and rehydration of oxides of aluminum[1] and silicon[2] have been thoroughly investigated, and anodic formation of oxide coatings on aluminum metal is also well studied.[3] Less well established is the preparation of oxidized and hydroxylated layers on the metals themselves.[4] In addition, a detailed understanding of reactivity of these layers with protolytically labile organometallics, a topic of interest for the design of surface modification organometallic chemical vapor deposition (OM-CVD) reagents, has not yet been accomplished.

We prepared reactive surfaces on aluminum and silicon powders and thin films by treating native surface oxide layers with water under varied conditions of oxidative hydroxylation vigor. To understand details of surface modification by reaction with such activated metal surfaces, these hydroxylated oxide surface layers of silicon and aluminum were treated with exemplars of two classes of organozirconium species: tetraneopentyl- and tetra-*tert*-butoxyzirconium. For the alkyl, proton transfer to a Zr-C bond is a reasonable protonolysis pathway; for the alkoxide, proton transfer either to Zr–O or to a lone electron pair on the oxygen is possible. In both cases deposition reactions were spontaneous and rapid, going to completion in less than an hour at room temperature. Measuring rates of such fast reactions can be particularly difficult for heterogeneous systems: The opacity of the substrates used in this work precluded most *in situ* optical spectroscopic methods, while the metallic nature of the aluminum eliminated NMR techniques, at least for that system. In addition, the surface area of our substrates was small, *ca.* 0.2 $m^2 \cdot g^{-1}$ (for the aluminum powder), and therefore, total measured hydroxyl content per gram was small, on the order of 10 $\mu mol \cdot g^{-1}$. Surface deposition studies were further complicated by the water-sensitive nature of the free metal complexes, the surface-bound complexes, and the metallic substrate itself; at the micromole level, even small amounts of adventitious water become a significant source of error. Also, there was no convenient quenching reaction for either reactant that would not also degrade the surface-bound complexes. Fortunately, a gravimetric technique, the quartz crystal microbalance (QCM),[5] enabled us to directly monitor the course of surface deposition reactions using thin films of each metal and to extract both stoichiometric and rate data employing common gas- and solution-phase surface-modification methodologies.

Experimental Section

General. Gas analyses were accomplished using a Hewlett-Packard Model 5840A gas chromatograph (for yields of volatile reaction products) or a Hewlett-Packard Model 5992B GC/MS (deuterium incorporation), equipped with 1% SP-1000 on 60/80 Carbopack B (Supelco) or 0.19% picric acid on 80/100 Carbopack C (Supelco) packed columns. Proton NMR spectra were obtained using either a JEOL GSX-270 or a General Electric QE-300 spectrometer. Scanning electron microscopy was performed on a JEOL JSM-780; no special preparation of the samples was necessary. Manipulation of all powdered metallic samples, freshly deposited aluminum electrodes, and organozirconium reagents was carried out in a nitrogen-filled Vacuum Atmospheres glovebox or under dry, oxygen-free nitrogen using standard Schlenk techniques. Gas manipulations were done on a high-vacuum manifold equipped with oil-diffusion and Töpler pumps and a calibrated manometer.

Water (HPLC grade) and D_2O (CIL, 99.9 atom % D) were degassed by performing several freeze–pump–thaw cycles. Diethyl ether was distilled from sodium benzophenone ketyl. *n*-Pentane was distilled from CaH_2 and was degassed before use (GC analysis showed <0.01% neopentane). Solvents were tested for dryness before use by adding a

⊛ Abstract published in *Advance ACS Abstracts,* August 15, 1993.

(1) Peri, J. B. *J. Phys. Chem.* **1965**, *69*, 211. Wefers, K.; Bell, G. M. *Oxides and Hydroxides of Aluminum*; Alcoa Research Laboratories: East St. Louis, IL, 1972.

(2) McDonald, R. S. *J. Am. Chem. Soc.* **1957**, *79*, 850; *J. Phys. Chem.* **1958**, *62*, 1168. Fischer, H. E.; King, S. A.; Miller, J. B.; Ying, J. Y.; Benziger, J. B.; Schwartz, J. *Inorg. Chem.* **1991**, *30*, 4403.

(3) Alwitt, R. S.; Dyer, C. K. *Electrochim. Acta* **1978**, *23*, 355. Vedder, W.; Vermilyea, D. A. *Trans. Faraday Soc.* **1969**, 561.

(4) (a) Some exceptions for aluminum include the following: Takahashi, H.; Yamagami, M.; Furuichi, R.; Nagayama, M. *Report of the Research Group for Functionalizing Aluminum and Its Surface Films*; The Light Metal Educational Foundation: Osaka, 1988. Krueger, W. H.; Pollack, S. R. *Surf. Sci.* **1972**, *30*, 263. Krueger, W. H.; Pollack, S. R. *Surf. Sci.* **1972**, *30*, 280. Zhuravlev, V. A.; Zakharov, A. P. *Dokl. Akad. Nauk SSSR* **1980**, *252*, 1162. (b) For silicon: Irene, E. A. *J. Electrochem. Soc.* **1978**, *125*, 1708. Wolters, D. L. *Inst. Phys. Conf. Ser.* **1980**, *No. 50*, 18. Russo, N.; Toscano, M.; Barone, V.; Lelj, F. *Surf. Sci.* **1987**, *180*, 599. Ibach, H.; Wagner, H.; Bruchman, D. *Solid State Commun.* **1982**, *42*, 457.

(5) (a) Miller, J. B.; Schwartz, J. *Inorg. Chem.* **1990**, *29*, 4579. (b) Miller, J. B.; Schwartz, J. *Acta Chem. Scand.* **1993**, *47*, 292.

0002-7863/93/1515-8239$04.00/0

drop of sodium benzophenone ketyl/tetraglyme solution to a *ca.* 5 mL aliquot of the solvent; a solvent was considered dry if the blue color persisted for a few minutes. Tetraneopentylzirconium,[6] prepared from neopentyllithium and $ZrCl_4$, was sublimed (50 °C, 10^{-3} Torr) prior to use and was stored in the dark at −40 °C. Tetra-*tert*-butoxyzirconium (Aldrich) was distilled (74 °C, <0.1 Torr) prior to use and was stored in the dark.

Preparation of Hydroxylated Metal Powders. All experiments were performed using 200-mesh aluminum (Aldrich, 99.99%) or 60-mesh silicon (Aldrich, 99.999%). The powders were received packed under nitrogen and were opened and manipulated in the drybox prior to any treatment, as for any air-sensitive reagent. Each of the following treatments typically lasted 18 h. Atmospheric exposure was performed at *ca.* 21 °C and at a typical relative humidity of >70%. Liquid water exposure was performed by placing an aliquot of the metal powder into a large excess of deionized water at *ca.* 21 °C and stirring. The slurry was then filtered and dried in air at 85 °C. Steam treatment was performed by placing the metal powder into a side-arm shoulder flask[7] attached to a small sample vial containing about 0.75 mL of degassed, distilled water (or D_2O). The two volumes were separated by a high-vacuum PTFE valve. The flask was sealed with a ball-to-ball adapter and evacuated to 10^{-2} Torr. The separating valve was then opened and the entire apparatus placed into an 85 °C oven. After treatment, the valve separating the flask and vial was closed and the large flask quickly evacuated while still hot. All samples were dried under vacuum at *ca.* 85 °C after their respective treatments. The appearance of the gray-purple silicon powder did not change after any treatment. Both the H_2O- and D_2O-steam-treated aluminum powders appeared darker when compared to the gray-silver atmosphere- and liquid-water-treated Al powders.

Hydroxyl Group Titration[5a] of Oxided Bulk Aluminum. Methyllithium (*ca.* 20 mL, Aldrich, 1.4 M in Et_2O) was placed in a vial and degassed. This vial was then attached to a flask containing the atmosphere-exposed aluminum sample (10.0 g, Aldrich, 99.99%) to be titrated, and the ensemble was evacuated. The methyllithium solution was added to the metal, and the slurry was stirred for 45 min. The slurry was then cooled to −78 °C and the evolved methane (0.07 mmol) Töpler pumped (2–3 h) through a trap (at −196 °C) into the calibrated manometer. Steam-treated aluminum powder (10.0 g) was similarly titrated to yield 0.24 mmol of methane.

Diffuse Reflectance Infrared Fourier Transform (DRIFT) Spectroscopy. Diffuse reflectance spectra were obtained using a Nicolet 740 FT-IR equipped with a Spectra Tech diffuse reflectance attachment. A nitrogen-purged glovebag was taped over the sample introduction door to allow manipulation of air-sensitive samples. Unless otherwise noted, the background sample was powdered KBr which had been dried overnight at 150 °C and 10^{-2} Torr.

Measurement of Relative Surface Areas of Aluminum Powders. Surface areas were measured by the BET method using N_2 as the adsorbent. Adsorption and desorption were measured using a thermal conductivity (TC) detector equipped Perkin-Elmer 3920 gas chromatograph. The sample (typically 4 g) was placed in a U-tube and purged for 30 min with a flow of *ca.* 2% N_2 in He, adjusted using flow meters. The overall flow was initially adjusted to eliminate an influx of atmosphere into the apparatus upon cooling; the same total flow was used for all experiments. The U-tube was immersed in liquid nitrogen until several minutes after the TC detector had returned to base line. The nitrogen bath was then removed and the apparatus allowed to warm to room temperature. Both adsorption and desorption peaks were detected. For analysis, the desorption peaks were integrated by weighing the peaks and those results were averaged.

Auger Analysis of Hydroxylated Thin Films. Quartz crystals were coated with *ca.* 2000 Å aluminum (99.999%, Aesar) using an Edwards Coating System E306A at $<10^{-6}$ Torr. Silicon (1200 Å) was deposited onto the surface of the crystals by Dr. Yehuda Aryeh at the David Sarnoff Research Center (Princeton). After the films had been hydroxylated as for the metal powders above, they were placed into an ultrahigh-vacuum (UHV) chamber. Pump-down to a base pressure of $<5 \times 10^{-8}$ Torr was achieved without bake-out to eliminate contamination of the samples. The chamber, fully described elsewhere,[8] was equipped with a Perkin-Elmer Φ 15-255GAR double-pass cylindrical mirror analyzer with an integral electron gun controlled by a Perkin-Elmer Φ 11-010 electron gun control. The primary electron energy was 2 keV with an emission current of 1.2 mA. Care was taken to ensure that the sample current was constant (Al, 3.2 μA; Si, 4 μA) and consistent between spectra. Spectra were obtained in the first-derivative mode $[dN(E)/dE]$ with a peak-to-peak modulation of 3 eV. The signal was detected with a Princeton Applied Research Model 128 A lock-in amplifier at a sensitivity of 1 mV, and the data were collected by laboratory computer. Spectra were measured twice at three different positions on the crystal electrode surface and individual results averaged. For depth profiling, the crystals were bombarded with a focused 3-keV, 20-mA Ar^+ beam, generated using a Varian 981-2043 ion bombardment gun. Auger spectra were obtained after each bombardment.

Deposition[5a] of Tetraneopentylzirconium from Solution onto Surface-Hydroxylated Bulk Aluminum and Silicon Powders. Solid tetraneopentylzirconium was mixed with the hydroxylated bulk metal powder in a flask separated by a valve from a vial containing 5–10 mL of degassed pentane. The assembly was evacuated, and the separating valve was opened to allow the pentane into the flask. After stirring overnight, the organic materials were distilled and the neopentane yield was measured.

Determination of Deuterium Incorporation in Evolved Neopentane. Neopentane-d_1 was collected from the reaction of neopentyllithium[9] (*ca.* 100 mg) with D_2O(g). GC/MS analysis (for neopentane minus methyl; molecular ion not observed) showed m/z 57:m/z 58 = 0.49:1. Neopentane evolved from deposition of $Zr(C_5H_{11})_4$ onto D_2O-steam-treated aluminum powder was collected and analyzed by GC/MS, which showed m/z 57:m/z 58 = 0.49:1. Thus, deuterium incorporation into evolved neopentane was *ca.* 100%.

Deposition[5b] of Tetra-*tert*-butoxyzirconium from Solution onto Surface-Hydroxylated Bulk Aluminum and Silicon Powders. An aliquot of a $Zr(OC_4H_9)_4$ solution in ether was added to the metal powder. The resulting slurry was stirred for several hours, the organic materials were distilled, and the 2-methyl-2-propanol yield was measured.

Quartz Crystal Microbalance. Quartz crystals (5.5 MHz, AT-cut, fundamental mode and 5.0 MHz, AT-cut, overtone polished) were obtained from Valpey-Fisher and were cleaned before use by soaking first in concentrated, aqueous NaOH and then H_2SO_4, followed by copious rinsing, first with water and then with acetone. The crystals were then oven-dried. Electrodes were vapor-deposited onto the crystals using an Edwards Coating System E306A at $<10^{-6}$ Torr. In previous work,[5] electrodes were prepared as a 500-Å aluminum (Aesar, 99.5%) layer on a 1500-Å gold (Aldrich, 99.99%) layer on top of a 150-Å chromium (Aldrich, 99.5%) base. This proved to be unnecessary: Excellent electrodes were prepared as a single 2000–2500-Å aluminum layer deposited directly onto the quartz crystal. Silicon-coated crystals were prepared as a 1200-Å layer over the Al electrode pattern on one side of the crystal. Electrode overlap area was measured to be 0.27 cm^2. Deposition reactions could be performed on either one or two sides of the crystal, depending on the electrode materials and the experimental setup.

For gas-phase deposition of $Zr(C_5H_{11})_4$, the QCM was driven with either a home-built Clapp oscillator[6] or an Intellemetrics IL02 single crystal oscillator. Gas-phase $Zr(O\text{-}t\text{-}Bu)_4$ deposition and all depositions from solution were studied using a custom oscillator circuit (obtained from Dr. Michael D. Ward). In all cases the circuits were powered by a Hewlett-Packard 6234A dual-output power supply. The Intellemetrics circuit was separated from the supply by a 12.5-mH choke. The crystal frequency was measured using a Hewlett-Packard 5334B universal counter and recorded using a laboratory computer.

Gas-Phase QCM Reactors. Two different reaction cells were used for the gas-phase deposition experiments. The first of these[5] was designed to be used at pressures as low as 10^{-6} Torr, enabling reactions with relatively low vapor pressure ($<10^{-2}$ Torr) materials (Figure 1). This reactor exposes both crystal electrodes to the reactant gas, thereby effectively doubling the available signal. Valves were arranged to allow separate evacuation of the crystal chamber and the reactant sample bulb as well as evacuation during the deposition reaction.

A second cell (Figure 2) was designed for use when deposition onto only one electrode surface was required. This cell was not appropriate for pressures lower than about 10^{-2} Torr. However, it was quite useful for high vapor pressure reactants. It also allowed for either static or dynamic vacuum. The pressure on both sides of the crystal was equalized by the tubing connection; this eliminated possible artifacts from physical distortion of the crystal. The cold trap served the dual purpose of preventing contamination of the nonexposed electrode and acting as a

(6) Davidson, P. J.; Lappert, M. F.; Pearce, R. *J. Organomet. Chem.* **1973**, *57*, 269.
(7) Fischer, H. E. Ph.D. Thesis, Princeton University, 1991.
(8) Chang, T.; Bernasek, S. L.; Schwartz, J. *Langmuir* **1991**, *7*, 1413.
(9) Zook, H. D.; March, J.; Smith, D. F. *J. Am. Chem. Soc.* **1959**, *81*, 1617.

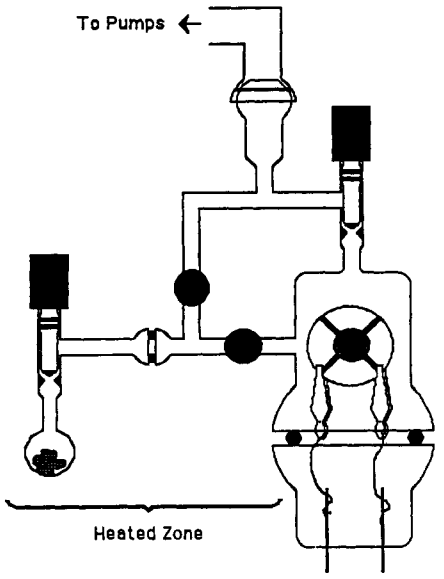

Figure 1. A low-pressure gas-phase QCM reactor.

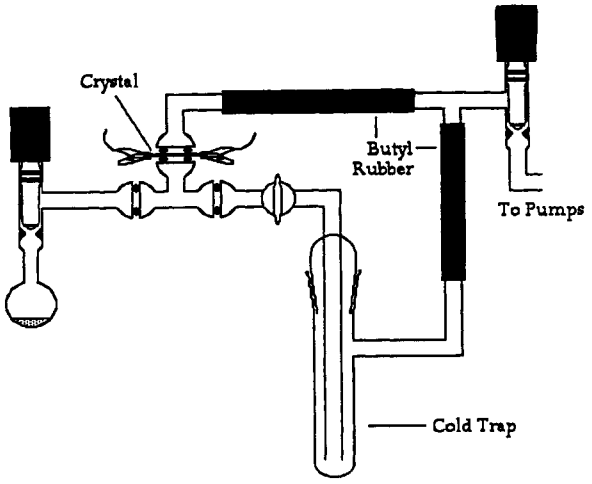

Figure 2. Another gas-phase QCM reactor.

cryopump for very volatile reactants (although caution must be exercised if liquid nitrogen is used as a cryogen under static vacuum).

Solution-Phase QCM Reactor. Depositions from solution were performed primarily in the reactor already described.[5] Syringes (SGE) used for the QCM solution-phase deposition had a spring-loaded metal-to-polytetrafluoroethylene (PTFE) sealing surface. To avoid air leaks around the needles during injection of the metal-complex solutions, the syringe and nitrogen inlet line were clamped to the ring stand which was used to stabilize the QCM cell from unnecessary vibrations. Nitrogen flow was kept to a minimum to avoid evaporating the solvent and hence cooling the crystal.

QCM-Monitored Gas-Phase Deposition of Tetraneopentylzirconium onto Surface-Hydroxylated Aluminum Films. Tetraneopentylzirconium (*ca.* 150 mg) was placed in a small vial, which was then attached to a reactor containing an electrode-deposited quartz crystal held by spring clips (Figure 1). The reagent vial was wrapped with heating tape and covered with glass wool and aluminum foil for insulation. The crystal chamber was evacuated. The heated zone was warmed to 50–60 °C under vacuum (10^{-4} Torr); temperature was monitored *via* a thermocouple or thermometer. After a short time (3–5 min), the vapor of the zirconium reagent was allowed into the crystal-containing chamber while the crystal frequency was monitored (1-Hz sampling rate, typical). The crystal chamber was continuously evacuated using the diffusion pump during and after exposure. The crystal frequency was monitored, even after exposure, to ensure that no further mass changes occurred, indicating that all changes observed were due to the deposition reaction and not to simple sublimation.

QCM-Monitored Deposition of Tetraneopentylzirconium from Solution onto Surface-Hydroxylated Aluminum and Silicon Films. The crystal was clamped between two 7-mm O-ring connectors under dry, oxygen-free N_2, and 0.5–1 mL of dry *n*-pentane was placed on the crystal in order to eliminate mass changes due to solvent effects.[8] The crystal frequency was monitored before and after a 0.5-mL aliquot of 0.05 M $Zr(C_5H_{11})_4$ in pentane was added all at once *via* syringe.

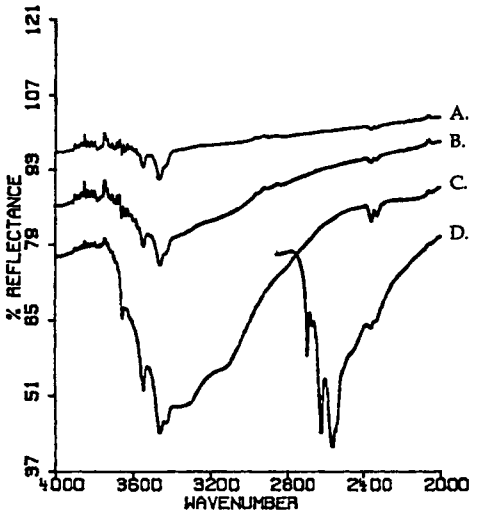

Figure 3. Hydroxyl region of the DRIFT spectra of Al powders oxidized by (A) ambient water, (B) liquid water, (C) steam, and (D) D_2O steam.

QCM-Monitored Gas-Phase Deposition of Tetra-*tert*-butoxyzirconium onto Surface-Hydroxylated Aluminum Films. Tetra-*tert*-butoxyzirconium (*ca.* 500 mg) was placed in the small vial of the reactor depicted in Figure 1. The reagent vial was immersed in an oil bath, and the delivery tube was wrapped with heating tape. Insulation was not necessary. The heated zone was warmed to 75–80 °C under vacuum (10^{-2} Torr); temperature was monitored *via* a thermocouple or thermometer. After a short time (3–5 min), the vapor of the zirconium reagent was introduced into the crystal-containing chamber while the crystal frequency was monitored (1-Hz sampling rate). The crystal chamber was continuously evacuated using only a mechanical pump during and after exposure. The crystal frequency was monitored, even after exposure, to ensure that no further mass changes occurred, indicating that all changes observed were due to the deposition reaction and not to simple condensation.

QCM-Monitored Deposition of Tetra-*tert*-butoxyzirconium from Solution onto Surface-Hydroxylated Aluminum and Silicon Films. The crystal was clamped between two 7-mm O-ring connectors under dry, oxygen-free N_2, and 1–2 mL of dry solvent was placed on the crystal. The crystal frequency was monitored before and after a 0.5-mL aliquot of 0.05 M $Zr(O\text{-}t\text{-}Bu)_4$ in ether was added all at once *via* syringe.

Results and Discussion

Surface Oxidation of Aluminum. Structural inferences for alumina surface OH groups have been discussed at length[10] on the basis of IR data; IR spectra for surface-oxidized aluminum metal (Figure 3) are similar to those reported for the oxide. Both isolated and hydrogen-bonded OH were noted. Each O–H mode appeared in spectra of Al treated with D_2O, which means that hydroxyl protons of the native oxide surface layer are labile to exchange. An apparent trend (Figure 3) is that as the vigor of hydroxylation increases, so does the relative intensity of the hydrogen-bonded absorptions. A simple scheme (Figure 4) suggests how surface hydroxyl content and distributions of types can be affected by reaction of water (or D_2O) with aluminum powders as a function of increasing vigor of treatment.

Surface hydroxyls of bulk alumina are fairly acidic ($pK_a \approx 9.2$[11]). Titration with methyllithium[12] provides a straightforward method for quantifying the degree of surface hydroxylation, producing 1 equiv of methane per OH. In this way, atmosphere-treated and steam-treated Al showed 7 μmol(OH)·g^{-1} and 24

(10) Knözinger, H.; Ratnasamy, P. *Catal. Rev.—Sci. Eng.* **1978**, *17*, 31.
(11) Robinson, McD.; Pask, J. A.; Fuerstenau, D. W. *J. Am. Ceram. Soc.* **1964**, *47*, 516.
(12) Hanke, W. *Z. Anorg. Allg. Chem.* **1973**, *395*, 193.

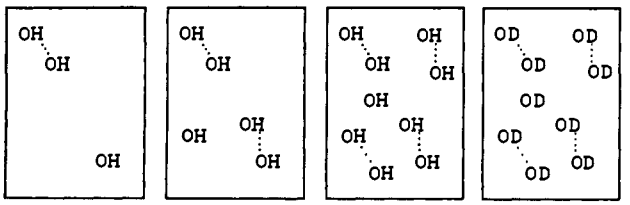

Figure 4. A schematic view of hydroxylated surfaces of Al or Si produced by reaction with water, showing how hydroxyl content and distribution of hydroxyl type could change with increasing vigor of treatment.

Table I. BET Surface Area Analysis of Some Standard, High Surface Area Oxides and Hydroxylated Aluminum Powders

sample	desorption (arb units)	nominal surf area ($m^2 \cdot g^{-1}$)	measd surf area ($m^2 \cdot g^{-1}$)
Degussa Aerosil-300 (SiO_2)	15239 ± 180	300	299
Degussa aluminum Oxid-C (Al_2O_3)	2255 ± 78	50	44.3
Degussa TiO_2 P-25	1577 ± 68	25	30.9
Al (atmosphere)	13.78 ± 0.35		0.15
Al (H_2O steam)	16.29 ± 1.02		0.20
Al (D_2O steam)	14.17 ± 0.83		0.16
blank	0.87 ± 0.08	6.3×10^{-5} m^2	0

μmol(OH)·g^{-1}, respectively. There are two ways in which the total hydroxyl content (per gram) could increase with increased vigor of oxidation: (1) a morphological change occurs resulting in a greater surface area or (2) a chemical enhancement of the surface hydroxyl concentration occurs for the powders. To examine the first possibility, powder surface areas were measured following mild or vigorous hydroxylation using an N_2 adsorption/desorption method (BET)[13] using three high surface area oxides of known area for calibration (Table I).[14] Although calibration points were obtained for higher surface area materials, *relative* surface area measurements may be meaningfully compared for these oxidized metals. Significantly, the surface areas of all of the variously treated aluminum powders were similar. The measured increase of only 33% in area between the atmosphere- and steam-treated powders cannot alone account for the measured 350% increase in hydroxyl group content measured by methyllithium titration.

Relative surface concentrations of oxygen and aluminum varied with changing hydroxylation conditions. Auger electron spectroscopy (AES) showed that the oxygen:aluminum ratio increased as the surface was more vigorously oxidized, consistent with an increase in the surface hydroxyl concentration. After correcting for elemental sensitivity,[15] the O:Al ratio for an evaporatively deposited Al film which had been exposed to air was 1.4 (±0.2), and the O:Al ratio for a steam-treated Al film was 1.9 (±0.2). These ratios correspond to the empirical formulas Al_2O_3 and "AlO_2" (or, perhaps more appropriately, AlOOH[16]), respectively.

The oxide layer of the steam-treated aluminum was found to be thicker than that of samples simply exposed to the atmosphere: Depth profiles of the elemental composition of the films were obtained by AES during bombardment with Ar^+ ions. AES were recorded [intensities of the O_{KLL} (512 eV) transition relative to the signal of the unbombarded surfaces and intensities of the Al transitions relative to those of oxygen] as a function of bombardment time (Figure 5a,b). The total amount of oxygen detectable by AES decreased for both films. The relative intensity of the interatomic transition $Al_{LVV'}$ (56 eV),[17] indicative of oxidized aluminum, remained flat, indicating that its absolute intensity was decreasing at about the same rate as that of oxygen. The transition for metallic aluminum, Al_{LMM} (68 eV), was not observed for either film until after long bombardment times. The large difference in the Al_{LMM}:O_{KLL} ratios observed for the two surfaces after long bombardment times indicates that the oxide layer is thicker for the steam-treated than for the atmosphere-treated metal. Perhaps this change in thickness is manifested in the small increase in surface area noted above.

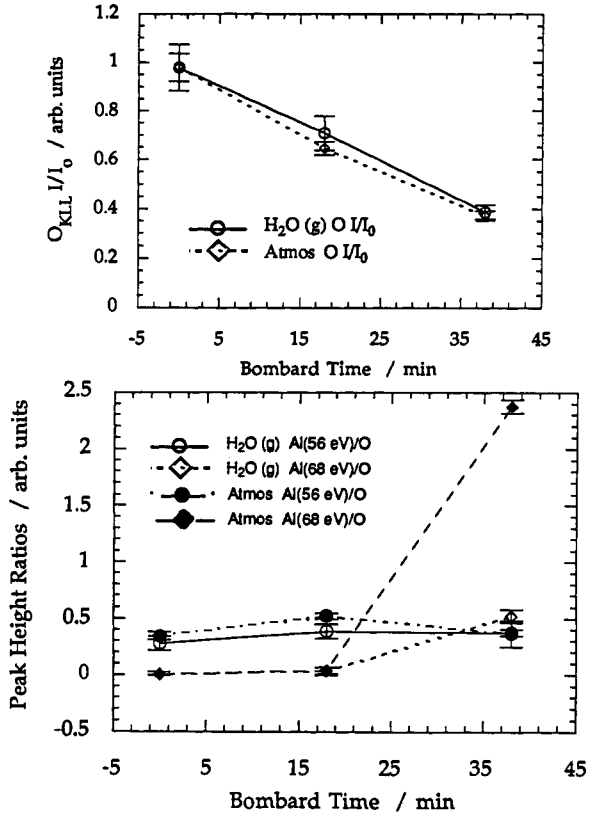

Figure 5. (A, top) Auger O_{KLL} intensity plotted against Ar^+ bombardment time. Signals have been normalized to the O_{KLL} signal of the unbombarded surface. (B, bottom) AES peak height ratios for oxidized aluminum films plotted against Ar^+ ion bombardment time.

Surface Oxidation of Silicon. A set of investigations similar to those for Al was carried out using powdered silicon. Treated powders were heated under vacuum to eliminate any adsorbed molecular water before DRIFT spectra were recorded. Water-treated Si showed OH and SiH bands (Figure 6); the latter appear at 2252 and 2102 cm^{-1}, for which assignment is based on single-crystal results.[18] Silicon treated with liquid water showed a modest increase in intensity in the hydroxyl region and a slight decrease in the surface SiH. The H_2O-steam-treated powder showed a large increase in all types of hydroxyls as well as some resolution of two types of hydrogen-bonded hydroxyls, not seen in bulk silica or in either of the less vigorously treated samples. The steam-

(13) After Brunauer et al.: Brunauer, S.; Emmett, P. H.; Teller, E. *J. Am. Chem. Soc.* **1938**, *60*, 309.

(14) Smooth, spherical particles of Al having a diameter of 0.127 mm (200 mesh) would have a surface area of 0.02 $m^2 \cdot g^{-1}$. We measured 0.2 $m^2 \cdot g^{-1}$ for Al as received. Although we lacked an appropriate standard for surface areas of these magnitudes and therefore the absolute values of the measured areas for the aluminum powders are not accurate, our observed area values are not unreasonable: milled Al is likely not smooth.

(15) Sensitivity factors used were obtained from the following: Davis, L. E.; McDonald, N. C.; Palmberg, P. W.; Rich, G. E.; Weber, R. E. *Handbook of Auger Electron Spectroscopy*; Perkin-Elmer Corporation: Eden Prairie, MN, 1979.

(16) This indicates the presence of hydroxyls on the surface. The IR spectra are consistent with a Bayerite surface layer (see ref 4).

(17) The prime (') indicates an orbital of a second atom. It should be noted that this peak may have the same energy as a bulk plasmon loss. See: Citrin, P. H.; Rowe, J. E.; Christman, S. B. *Phys. Rev. B* **1976**, *14*, 2642. Shiraki, Y.; Kobayashi, K. L. I.; Katayama, Y. *Surf. Sci.* **1978**, *77*, 449.

(18) Chabal, Y. J. *Phys. Rev. B* **1984**, *29*, 3677. Schmeisser, D.; Demuth, J. E. *Phys. Rev. B* **1986**, *33*, 4233.

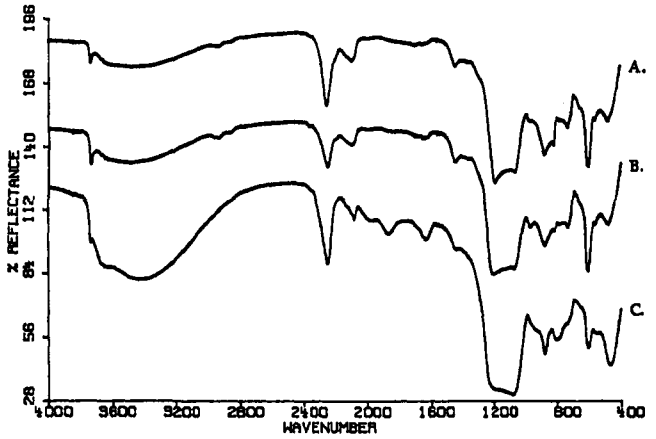

Figure 6. DRIFT spectra of Si powder oxidized by (A) ambient water, (B) liquid water, and (C) steam.

Table II. Tetraneopentylzirconium Loadings on Hydroxylated Aluminum and Silicon Electrode Surfaces as Determined by QCM

substrate	hydroxylation meth	cryst polish	loading ($ng \cdot cm^{-2}$)[c]	concn ($nmol \cdot cm^{-2}$)[d]
Al	atmosphere[a]	3 μm	1300	6
Al	H_2O(l)[a]	3 μm	2200	10
Al	H_2O steam[a]	3 μm	4800	21
Al	H_2O steam[a]	overtone	1300	5.6
Al	H_2O steam[b]	overtone	1200	5.2
Al	D_2O steam[a]	3 μm	5000	22
Si	H_2O steam[b]	3 μm	2500	11
Si	D_2O steam[b]	3 μm	2300	10

[a] Deposition from the gas phase. [b] Deposition from pentane solution. [c] Corrected for number of crystal sides on which deposition occurred. [d] For the surface-ligated fragment ZrR_2.

treated surface also showed an increase in the hydride stretch at 2252 cm^{-1} and the presence of oxide-like bands at 1978 and 1865 cm^{-1}, indicating the growth of a significantly thick SiO_x layer on the metal, which was not as apparent on the less vigorously treated surfaces.

Deposition of Tetraneopentylzirconium onto Hydroxylated Aluminum Metal. Tetraneopentylzirconium reacted with 2 equiv of appropriately activated Al surface hydroxyl to give a surface-bound dineopentylzirconium complex and 2 equiv of neopentane, the same stoichiometry as was found for the pure metal oxide.[19] The complex loading on atmosphere-exposed Al was determined by GC to be 3 $\mu mol \cdot g^{-1}$, and on H_2O-steam-treated Al 12 $\mu mol \cdot g^{-1}$ (based on Zr by neopentane evolution), in accord with methyllithium titration data assuming a deposition stoichiometry of two hydroxyls per Zr center (Table II). Mass spectrometric analysis of the evolved alkane produced by reaction of the deuteroxylated Al surface with tetraneopentylzirconium showed production of neopentane which was nearly 100% deuterium labeled. DRIFT analysis of reaction products showed the expected loss of intensity of both isolated and hydrogen-bonded OH stretching bands and the appearance of features expected for supported neopentylzirconium species[20] (Figure 7).

Deposition of Tetraneopentylzirconium onto Hydroxylated Silicon. Deposition of tetraneopentylzirconium onto hydroxylated

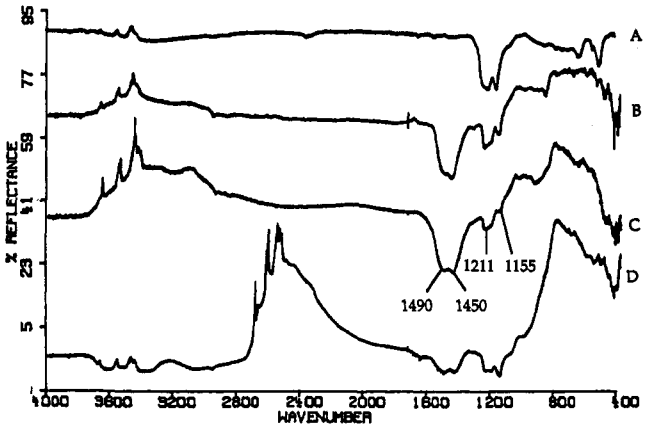

Figure 7. Ratioed DRIFT spectra of tetraneopentylzirconium deposited onto hydroxylated Al powders and the appropriate Al background spectrum: (A) atmosphere exposed, (B) H_2O(l) treated, (C) H_2O steam treated, and (D) D_2O steam treated. Ascending peaks are due to species depleted in the deposited samples relative to the unmodified surfaces.

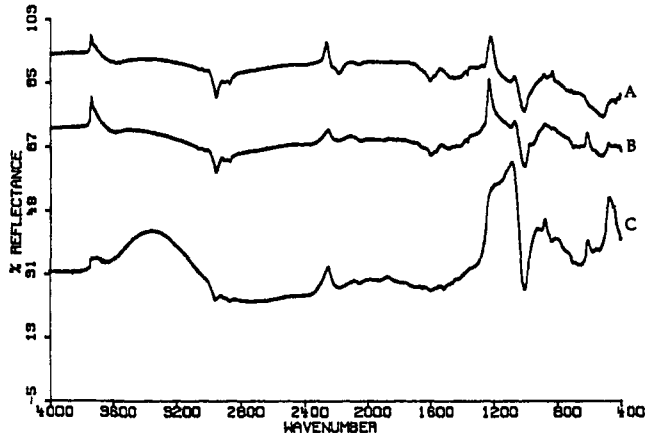

Figure 8. Ratioed DRIFT spectra of tetraneopentylzirconium deposited onto hydroxylated Si powders and the Si background spectrum: (A) atmosphere exposed, (B) H_2O(l) treated, (C) H_2O steam treated.

silicon powders also occurred with evolution of 2 equiv of neopentane, in accord with deposition onto silica. DRIFT spectra of the products of zirconium-complex deposition onto variously hydroxylated silicon surfaces were recorded (Figure 8) using the unreacted silicon powders as background. Deposition onto hydroxylated Si showed depletion in the OH region of the IR spectrum. The loss of the isolated ν_{OH} band at 3744 cm^{-1} was clearly evident, especially for the less vigorously treated surfaces, but loss of the broader, hydrogen-bonded bands was also apparent.[21] The Zr-modified surface also showed a loss of intensity in the δ_{SiOH} at 1225 cm^{-1}.

Kinetics of Tetraneopentylzirconium Deposition. Kinetics of gas-phase deposition onto variously hydroxylated aluminum electrode surfaces were monitored by QCM by noting the frequency change of a crystal as the metal complex reacted with the surface-hydroxylated crystal electrodes (Figure 9A). The difference between the initial and final frequencies for each surface reaction gives a direct gravimetric determination of the loading

(19) Schwartz, J.; Ward, M. D. *J. Mol. Catal.* **1980**, *8*, 465.

(20) The deposited complex shows very weak features appearing at 2950 and 2865 cm^{-1} from two of the ligand neopentyl C–H stretching modes. Due to low intensity, an intermediate-energy neopentyl C–H stretch is not observed. Two broad peaks at 1490 and 1450 cm^{-1} also appear in these difference spectra. While broadened, the higher energy peak might correspond to the CH_2 scissors mode of the neopentyl methylenes, which appears as two bands at 1480 and 1466 cm^{-1} in the unreacted complex, undoubtedly because the complex cannot be strictly tetrahedral, but is, at best, D_{2d}. The broad 1450-cm^{-1} peak is due to the δ_{CH_3} modes, which appear at 1394 and 1365 cm^{-1} in the unreacted complex. Note that, in each case, these bands are raised in energy relative to the free complex. The typical skeletal-vibration doublet bands of the *tert*-butyl moieties are observed as four bands in the unreacted complex at 1138, 1117, 1038, and 1018 cm^{-1}, probably due to the lowered symmetry of the complex. The corresponding bands of the deposited complex appear at 1211 and 1155 cm^{-1}, as highlighted in the difference spectra.

(21) The C–H region has a stronger signal and is better resolved than on the aluminum surface. All three of the neopentyl bands are observed, at 2955, 2908, and 2872 cm^{-1}. Interestingly, reaction with the zirconium complex seems to cause some depletion of the ν_{SiH} bands at 2252 and 2102 cm^{-1}. As for the Al surface, broad, unresolved ligand bands appear at *ca.* 1470 (CH_2 scissors) and 1400 cm^{-1} (δ_{CH_3}). Skeletal vibration bands are not observed due to strong absorption by the support in the region 1050–1250 cm^{-1}.

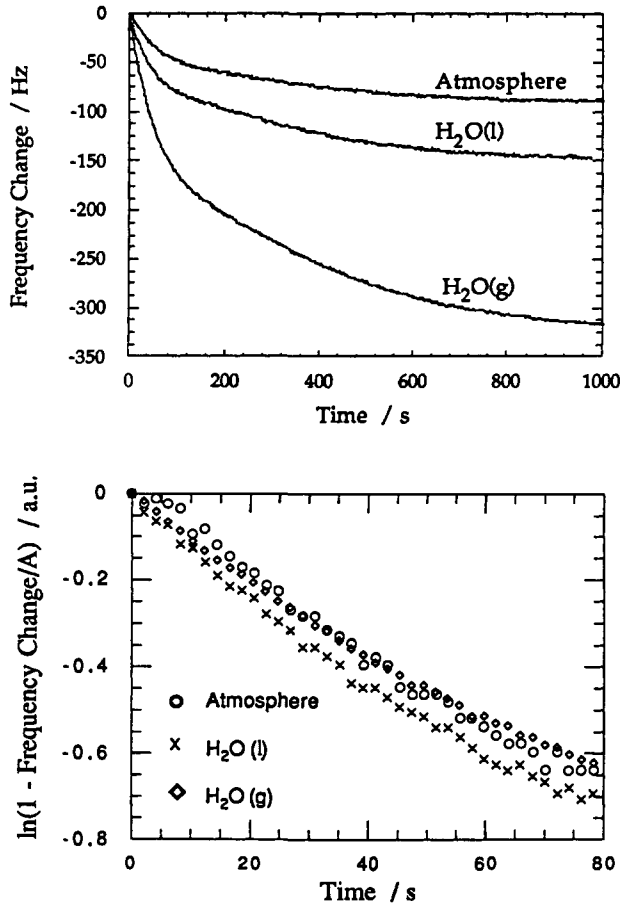

Figure 9. (A, top) Changes in QCM frequency as tetraneopentylzirconium reacts from the gas phase with the surface-hydroxylated aluminum crystal electrodes. (B, bottom) Semilog plots of changes in QCM frequency as tetraneopentylzirconium reacts from the gas phase with the surface-hydroxylated aluminum crystal electrodes.

of the organometallic.[22] By this measure, complex loading on steam-treated Al is 3.6 times that of the atmosphere-exposed metal. These results correlate well with complex loadings measured on similarly prepared metal powders (deposition yield for (steam-treated surface):(atmosphere-treated surface) = 35:1).

Depositions were performed under conditions of excess organometallic such that reactions were pseudo-first-order in surface hydroxyl groups, yielding a simple rate law:[23] $-d[OH]/dt = k_{obs}[OH]$. By plotting the crystal frequency change relationship[24] on a semilog scale against time, the observed rate constant, k_{obs}, may be obtained analytically as the slope of a line fitted to the data points (Figure 9B). Although the three differentially oxidized Al surfaces were found to have very different hydroxyl loadings and to react to give correspondingly different amounts of metal-complex surface loadings, observed rate constants for deposition onto all of the surfaces were nearly identical (Table II).

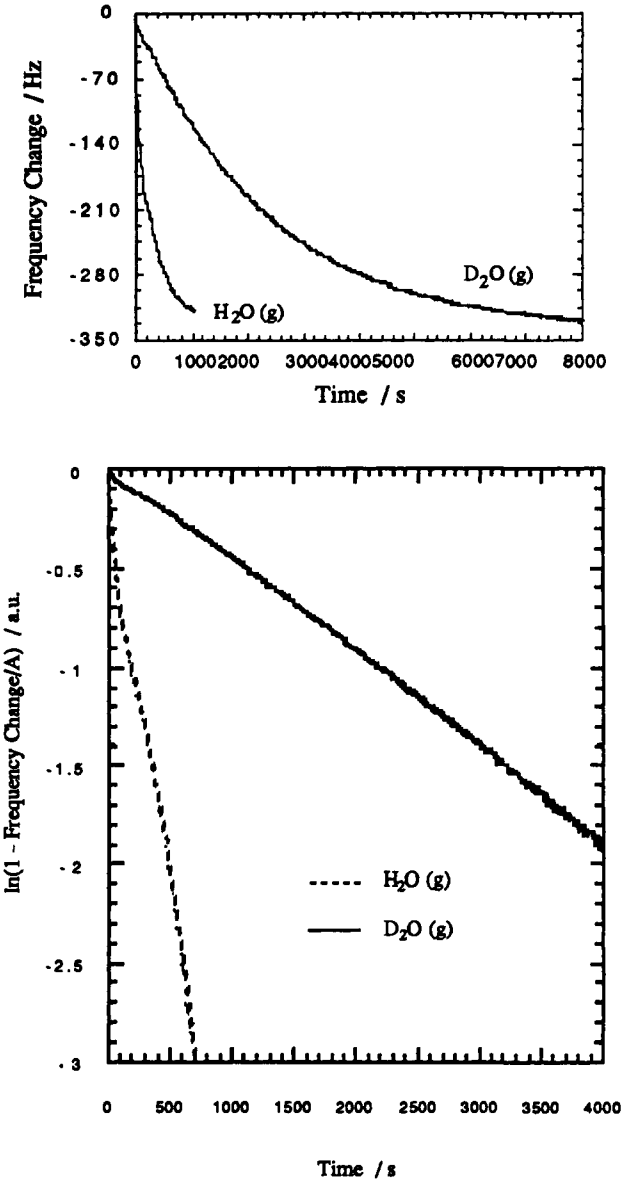

Figure 10. (A, top) Changes in QCM frequency as tetraneopentylzirconium reacts from the gas phase with H_2O- and D_2O-steam-treated aluminum crystal electrodes. (B, bottom) Semilog plot of changes in QCM frequency as tetraneopentylzirconium reacts from the gas phase with H_2O- and D_2O-steam-treated aluminum crystal electrodes.

Measured frequency changes for H_2O- *versus* D_2O-steam-treated Al surfaces, plotted against reaction time, showed total complex surface loadings to be similar (Figure 10A). However, observed deposition rate constants were dramatically different: Comparison of the two semilog plot slopes (Figure 10B) revealed a high observed kinetic isotope effect, $k_H/k_D = 8.4$.

The kinetics of tetraneopentylzirconium reaction with H_2O- and D_2O-steam-treated silicon were also monitored by QCM, accomplished by evaporatively coating one side of the quartz crystal electrode assembly with >1200 Å of silicon. Organometallic deposition was done on silicon substrates from pentane

(22) This assumes that the crystal surface topologies are similar. Rough surfaces have increased effective surface areas and, therefore, higher total loadings than smooth surfaces, even for similar *areal* loadings.

(23) Alternatively, the surface hydroxyl concentration, $C_{OH}(t)$, may be quantified in terms of the initial concentration, C_0, as

$$C_{OH}(t) = C_0 \exp(-k_{obs}t) \quad (1)$$

In terms of the concentration of reacted hydroxyls, $C_{OM}(t)$, this becomes

$$C_{OM}(t) = C_0(1 - \exp(-k_{obs}t)) \quad (2)$$

Mass increase is related to hydroxyl group reaction, and the Sauerbrey relationship,[24]

$$\Delta f = -f_0^2 \Delta m/(\rho_q \mu_q)^{1/2} \quad (3)$$

relates electrode mass change to the observed crystal frequency, $f(t)$. Thus,

$$f(t) - f(0) = A(1 - \exp(-k_{obs}t)) \quad (4)$$

where $A = f(\infty) - f(0)$. Rearranging eq 4 and substituting $\Delta f = f(t) - f(0)$ gives

$$\ln(1 - \Delta f/A) = -k_{obs}t \quad (5)$$

(24) Sauerbrey, G. *Z. Phys.* **1959**, *155*, 223.

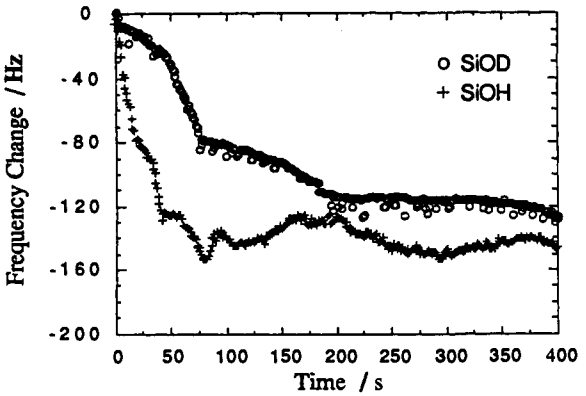

Figure 11. Changes in QCM frequency as tetraneopentylzirconium reacts in pentane solution with H_2O- and D_2O-steam-treated, silicon-coated electrodes.

Table III. Rate Data for the Deposition of Tetraneopentylzironium onto Hydroxylated Aluminum and Silicon

substrate	hydroxylation deposition meth	medium	k_{obs} (s^{-1})	k_H/k_D
Al	atmosphere	gas phase	$4.2(\pm0.3) \times 10^{-3}$	
Al	H_2O(l)	gas phase	$4.3(\pm0.3) \times 10^{-3}$	
Al	H_2O steam	pentane	$4.5(\pm0.6) \times 10^{-3}$	
Al	H_2O steam	gas phase	$3.7(\pm0.3) \times 10^{-3}$	
Al	D_2O steam	gas phase	$0.44(\pm0.02) \times 10^{-3}$	8.4(+1.0/−0.9)
Si	H_2O steam	pentane	$4.1(\pm0.5) \times 10^{-2}$	
Si	D_2O steam	pentane	$0.77(\pm1.5) \times 10^{-2}$	5.3(+2.1/−1.4)

solution and onto steam-treated electrode surfaces. Complex loadings were similar to those found for similarly treated Al (Table II), and as for Al, the observed kinetic isotope effect (from Figure 11) for this system was large: $k_H/k_D \approx 5.3$ (Table III). Although signal-to-noise problems inherent to solution-phase QCM experiments gave relatively larger errors in measurement for Si surface deposition, there is apparently no significant change in rate or mechanism with change in deposition technique[25,26] or substrate.

Protolytic cleavage of the alkyl–zirconium bond by a surface hydroxyl group likely involves initial coordination of the organometallic complex to the surface, either to a hydroxyl group oxygen or to a μ-oxo unit. Although protonolysis without such initial coordination could be argued in a solution–surface process, it seems unlikely for a gas-phase–surface procedure since charge-separated intermediates would be formed: $ZrR_4 + MOH \rightarrow [ZrR_3(RH)]^+ + MO^-$ (M = Al or Si). Since we have observed no significant differences in rates of complex–surface reaction using either dissolved or low-pressure vapor organometallic, it is reasonable that proton transfer occurs through similar mechanisms in both cases:

$$ZrR_4 + MOH \rightarrow MOH(ZrR_4) \rightarrow MOZrR_3(RH) \rightarrow MOZrR_3 + RH$$

Because the QCM technique is mass-sensitive, it can be used to determine whether initial coordination of the organometallic to the surface is reversible. In other words, if coordination were fast and irreversible, then an increase in mass for the QCM would be recorded for the adsorption step. However, coordination should have only a secondary kinetic isotope effect, and this should be small (for example $k_H/k_D \geq 1.05$). The large kinetic isotope effect, $k_H/k_D > 5$, measured for tetraneopentylzirconium reaction with hydroxylated Si or Al indicates that proton transfer is rate-limiting and that surface coordination is reversible (Scheme I).

(25) Signal-to-noise problems inherent to the solution-phase deposition route were compounded by the use of smooth, "overtone-polished" crystals, which have a low effective surface area and hence an inherently lower signal.
(26) Miller, J. B. Ph.D. Thesis, Princeton University, 1992.

The large value for k_H/k_D is interpreted to mean that $k_2 \ll k_{-1}$: In this scheme, the only reasonable protonation site available in the surface–(tetraneopentylzirconium) complex is the Zr–C σ-bond. While proton transfer to this site is thermodynamically highly favorable, it appears to be kinetically not so propitious. Once the Zr–C bond is protonated, however, it is likely that the resulting η^2-neopentane is lost rapidly. (The loss of the second equivalent of alkane would not be independently discernible by the QCM method.)

Deposition of Tetra-*tert*-butoxyzirconium onto Hydroxylated Aluminum and Silicon. To test the hypothesis that the *kinetic* basicity of the ligand (and not necessarily the thermodynamic basicity) dominates the deposition sequence, the reactions of tetra-*tert*-butoxyzirconium with oxidized Si and Al were studied. This alkoxide is structurally similar to tetraneopentylzirconium, although the lone electron pairs on the oxygen atoms certainly change details of metal–ligand bonding. Most importantly, the lone pairs on oxygen or Zr–O π-bonds would provide an alternate, and perhaps kinetically more favorable, site for proton transfer to the metal complex than the σ-bond of the tetraalkyl.

Tetra-*tert*-butoxyzirconium reacted with surface-hydroxylated aluminum metal producing 2 equiv of *tert*-butyl alcohol, just as on alumina. Unlike tetraneopentylzirconium for which the yield of evolved alkane scaled with the surface hydroxyl content as determined by methyllithium titration, deposition loadings of the alkoxide complex were not so directly related. For example, the loading of the alkoxide complex on H_2O-steam-treated Al was 10 μmol·g^{-1}, slightly less than the loading of the alkyl complex onto aliquots of the same support, and loading on Al metal exposed to the atmosphere was 1 μmol·g^{-1}. In contrast to results obtained using the alkylzirconium, alkoxide complex loading was about one-third what would be predicted on the basis of the methyllithium-determined hydroxyl titer[27] (Table IV). Tetra-*tert*-butoxyzirconium also reacts with surface-hydroxylated silicon metal, producing 2 equiv of *tert*-butyl alcohol, and reaction with the zirconium alkoxide complex seems to cause a depletion of the ν_{SiH} intensity at 2252 and 2102 cm^{-1} (Table IV).[28]

Kinetics of Tetra-*tert*-butoxyzirconium Deposition. The kinetics of gas-phase deposition of tetra-*tert*-butoxyzirconium complex onto variously hydroxylated aluminum electrode surfaces were monitored by QCM. Complex loading on the steam-treated surface was 5.7 times that of the atmosphere-exposed surface, in reasonable accord with stoichiometric measurements made for the differently treated bulk metal powders. Rate constants for complex deposition onto the differently hydroxylated aluminum surfaces were similar (but the small total frequency change for deposition onto atmosphere-treated Al resulted in scatter in the semilog plots for that case). Significantly, observed rates for deposition of the (thermodynamically) relatively low basicity tetraalkoxide were an order of magnitude *greater* than those measured for the (thermodynamically) relatively highly basic tetraalkyl. When deposition rates were measured for H_2O- and D_2O-steam-treated surfaces (Figure 12), it was found that $k_H/k_D = 1.7$ (Table V).

(27) One major difference between the atmosphere-exposed and steam-treated surfaces is the distribution of the types of hydroxyls; on the steam-treated surface mainly hydrogen-bonded OH groups are present, while on the atmosphere-exposed surface a greater proportion of isolated OH groups exist. It may be that deposition of the alkoxide complex has some reactivity preference for the more acidic hydrogen-bonded hydroxyls.
(28) Deposition products were examined by DRIFT using the unmodified surface as a background. Selected spectroscopic data for the deposition of tetra-*tert*-butoxyzirconium onto hydroxylated Al and Si are shown below.

assignment	$Zr(O\text{-}t\text{-}Bu)_4$	Al	Si
ν_{CH} (cm^{-1})	2970	2972	2978
δ_{CH_3} (cm^{-1})	1359, 1383	1364, 1383	1371, 1395
skeletal vibrations (*t*-Bu) (cm^{-1})	1225	1228	1242
ν_{CO} (cm^{-1})	1192	1205	1153

Scheme I. Reversible Coordination of the Complex Precedes Proton Transfer ($k_2 \ll k_{-1}$)

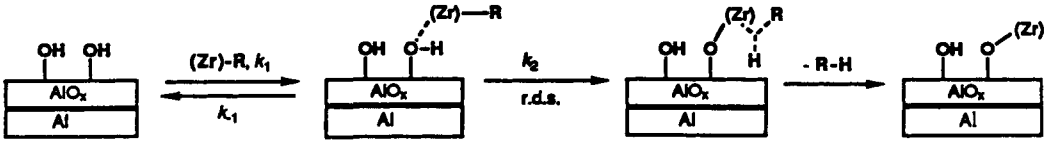

Scheme II. Reversible Coordination of the Complex Precedes Proton Transfer ($k_2 \leq k_{-1}$).

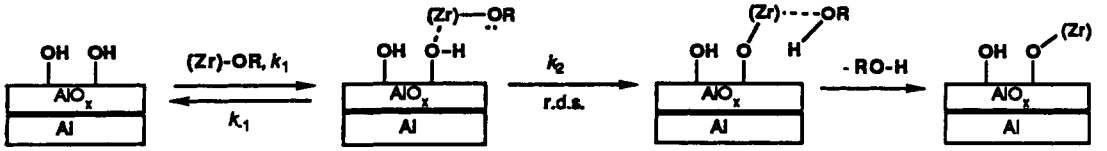

Table IV. Tetra-*tert*-butoxyzirconium Loadings on Hydroxylated Aluminum and Silicon Electrode Surfaces

substrate	hydroxylation meth	crystal polish	loading ($ng \cdot cm^{-2}$)[c]	concn ($nmol \cdot cm^{-2}$)[d]
Al	atmosphere[a]	overtone	250	1.1
Al	H_2O steam[a]	3 μm	4200	18
Al	H_2O steam[a]	overtone	1800	7.5
Al	H_2O steam[b]	overtone	1700	7.2
Al	D_2O steam[a]	3 μm	4200	18
Si	H_2O steam[b]	overtone	550	2.3
Si	D_2O steam[b]	overtone	550	2.3

[a] Deposition from the gas phase. [b] Deposition from diethyl ether solution. [c] Corrected for number of crystal sides on which deposition occurred. [d] For the surface-ligated fragment $Zr(OR)_2$.

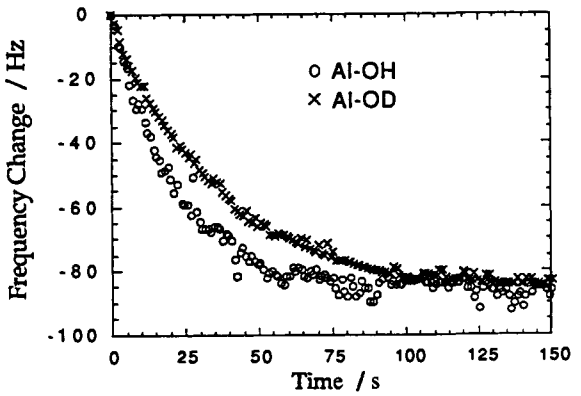

Figure 12. The changes in frequency of the QCM as gas-phase tetra-*tert*-butoxyzirconium reacts with the H_2O- and D_2O-steam-treated aluminum electrodes on the crystals.

Finally, the kinetics of the reaction of a diethyl ether solution of tetra-*tert*-butoxyzirconium with H_2O- and D_2O-steam-treated silicon were monitored by QCM. Although hampered by unfavorable signal-to-noise problems, it was possible to make the qualitative observation that the two surface loadings were similar, on the basis of the final frequency changes.[24] The observed kinetic isotope effect was small, $k_H/k_D \approx 1.5$ (Table V).

The small kinetic isotope effect observed for tetra-*tert*-butoxyzirconium implies a mechanistic difference for the proton-transfer step compared with tetraneopentylzirconium. Two interpretations are reasonable to explain the relatively small isotope effect measured. The first is that the observed isotope effect is secondary, in which coordination of the tetra-*tert*-butoxyzirconium to a surface hydroxyl is rate-limiting. The second is that the isotope effect is, in fact, primary, but small, which we interpret to mean the rate of proton transfer is comparable to the rate of decoordination of the complex from the surface (or, $k_{-1} \approx k_2$ in Scheme II),[29-31] assuming comparable proton-transfer geometries in both cases. This interpretation also

(29) Melander, L.; Saunders, W. H., Jr. *Reaction Rates of Isotopic Molecules*; Wiley: New York, 1980; p 158ff.

Table V. Rate Data for the Deposition of Tetra-*tert*-butoxyzirconium onto Hydroxylated Aluminum and Silicon

substrate	hydroxylation meth	deposition medium	k_{obs} (s^{-1})	k_H/k_D
Al	atmosphere	gas phase	$4.9(\pm0.9) \times 10^{-2}$	
Al	H_2O steam	Et_2O	$4.9(\pm0.3) \times 10^{-2}$	
Al	H_2O steam	gas phase	$5.2(\pm0.2) \times 10^{-2}$	
Al	D_2O steam	gas phase	$3.1(\pm0.2) \times 10^{-2}$	1.7(±0.2)
Si	H_2O steam	Et_2O	$2.8(\pm0.4) \times 10^{-2}$	
Si	D_2O steam	Et_2O	$1.9(\pm0.3) \times 10^{-2}$	1.5(+0.5/−0.4)

explains the relatively fast deposition of the tetraalkoxide relative to the tetraalkyl: It supports the hypothesis that lone pairs on oxygen or Zr–O π-bonds[32] can provide an alternate, kinetically favorable site for proton transfer to a metal complex relative to the σ-bond of the tetraalkyl. (Just as was the case for alkyl complex deposition, the second proton-transfer step cannot be directly discerned by the QCM technique.) Significantly, observed rates for deposition of tetra-*tert*-butoxyzirconium were *ca.* an order of magnitude *greater* than those measured for tetraneopentylzirconium. A simple prediction based solely on considerations of thermodynamic basicity might have suggested the alkyl to be the more reactive deposition reagent.

Conclusions

Surfaces of aluminum and silicon metal powders and thin films can be both oxidized and hydroxylated by reaction with water without grossly changing surface areas. The depth of the oxidation layer and the amount of surface hydroxylation correlate with the vigor of the water treatment conditions. The distribution of types of surface hydroxyl groups also depends on reaction conditions; hydrogen-bonded hydroxyls are relatively more prevalent on surfaces which were treated more vigorously. Since these hydroxyl groups provide chemical sites for anchoring a protolytically labile organometallic complex, controlling the hydroxylation profile can be a possible first step in enabling protection of or enhancing adhesion to a metallic surface on the molecular level.

Water-hydroxylated surfaces of Al and Si were used as protolytic deposition substrates for tetraneopentylzirconium and gross structurally related tetra-*tert*-butoxyzirconium. The stoichiometry of deposition was the same for both complexes and for

(30) The fractional magnitude of the isotope effect, compared with its maximal, intrinsic amount, has been related to the "sensitivity index" for the isotopic step in a multistep process: The more the overall reaction rate depends on the isotopic step (the higher the sensitivity of the reaction rate to that step), the larger the fractional magnitude will be. See: Ray, W. J., Jr. *Biochemistry* **1983**, *22*, 4625.

(31) An alternative explanation, that deposition and proton transfer are both fast and reversible and alcohol desorption is rate-limiting, seems less reasonable: The isotope effect for alcohol (ROH *versus* ROD) desorption would be expected to be very small.

(32) For examples of Zr–O π-bonding, see: Lubben, T. V.; Wolczanski, P. T.; Van Duyne, G. D. *Organometallics* **1984**, *3*, 977. Clark, J. F.; Drew, M. G. B. *Acta Crystallogr.* **1974**, *B30*, 2267. Hunter, W. E.; Hrncir, D. C.; Bynum, R. V.; Penttila, R. A.; Atwood, J. A. *Organometallics* **1983**, *2*, 750.

each surface, and the amount of surface-complex formation was dependent on the vigor of the metal hydroxylation conditions. Overall, deposition yields for hydroxylated metal surfaces were found to be similar to those observed previously on metal oxides.

The mass-sensitive QCM technique was used to probe the kinetics of surface-complex reactivity. Significantly, observed rates for deposition of the tetraalkoxide were an order of magnitude *greater* than those measured for the tetraalkyl. When deposition rates were measured for H_2O- and D_2O-steam-treated surfaces, a large kinetic isotope effect, $k_H/k_D \approx 8.4$, was found for the tetraalkyl; a smaller kinetic isotope effect, $k_H/k_D = 1.7$, was measured for the tetraalkoxide. These data indicate that the reaction between a hydroxylated metal surface and an organometallic complex proceeds by reversible coordination of the metal complex to the hydroxylated surface, followed by rate-determining proton transfer and subsequent loss of the protonated ligand. Thus, the less basic tetraalkoxide is favored over the more basic tetraalkyl, ratewise, because lone pairs on oxygen or Zr–O π-bonds can provide *kinetically* favorable sites for proton transfer to a metal complex relative to the σ-bond of an alkyl.

Acknowledgment. The authors acknowledge the National Science Foundation for support of this research. They also thank Prof. Michael D. Ward for help with QCM technology and Prof. Robert A. Pascal, Jr., for discussions of isotope effects.

Supplementary Material Available: Infrared spectra, tables of IR data, and plots of QCM data (15 pages). Ordering information is given on any current masthead page.